

POLYPROPYLENE – ZINC OXIDE NANOROD HYBRID MATERIAL FOR APPLICATIONS IN SEPARATION PROCESSES

Szymon Jakubiak^{*1}, Justyna Tomaszewska¹, Anna Jackiewicz², Jakub Michalski¹,
Krzysztof J. Kurzydłowski¹

¹Faculty of Materials Science and Engineering, Warsaw University of Technology, Wołoska Str.
141, 02-507 Warsaw, Poland

²Faculty of Chemical and Process Engineering, Warsaw University of Technology, Waryńskiego
Str. 1, 00-645 Warsaw, Poland

Hybrid filter material was obtained via modification of polypropylene (PP) nonwoven with nano-size zinc oxide particles of a high aspect ratio. Modification was conducted as a three-step process, a variant of hydrothermal method used for synthesis of nano-ZnO, adopted for coating three dimensional polymeric nonwoven filters. The process consisted of plasma treatment of nonwoven to increase its wettability, deposition of ZnO nanoparticles and low temperature hydrothermal growth of ZnO rods. The modified nonwovens were investigated by a high resolution scanning electron microscopy (HR-SEM). It has been found that the obtained hybrid filters offer a higher filtration efficiency, in particular for so called most penetrating particle sizes.

Keywords: filter materials, nanomaterials, ZnO nanorods

1. INTRODUCTION

Fibrous filters are commonly used for air and water purification in the European market worth 1.5 billion Euro a year (Sutherland et al., 2011). In particular, such filters are utilized in single step processes or as pre-filters in multi-step installations. With good efficiency, high capacity of removing solid matter and low operation costs they are often much better choice than other filtration systems. However, they also exhibit some disadvantages which limit their applications. One of them is a phenomenon of a minimum filtration efficiency for sub-micron particles due to the differences in trapping mechanisms for nano- and micro-scale solids. As a result, particles with the size ranging between 0.1 and 0.5 μm , in so called most penetrating particle size (MPPS) region, are removed with a lower rate, stimulating research and development efforts aiming at designing higher performance filters. Along these lines of research, it was proven that fibres with sub-micrometric diameters exhibit higher filtration efficiency for MPPS (Podgórski et al., 2006). However, sub-micrometric fibres increase the pressure drop and shorten operation time, thus bringing about a higher cost (Jackiewicz et al., 2013).

In the present paper we describe an alternative approach to increasing the efficiency of filtering of MPPS, which is based on the filter modification with zinc oxide (ZnO) nanoparticles of high aspect ratio, in-situ synthesized using a hydrothermal method. The hydrothermal methods in the past have been widely used to deposit ZnO nano-particles on flat surfaces such as glass or silica plates

*Corresponding author, e-mail: szymon.jakubiak@inmat.pw.edu.pl

(Choi et al., 2012; Kenanakis et al., 2012; Kwon et al., 2011). In this study, it was adapted to deposit ZnO rods on highly porous nonwoven filter material.

It should be noted in the context of the undertaken research efforts that ZnO exhibits a whole range of promising properties, which can be utilized in optoelectronic applications (Chen et al., 2009), in sensors (Ates et al., 2013; Minh et al., 2013; Yin et al., 2014), light conversion (Baek et al., 2012; Nayeri et al., 2013), and drug delivery (Zhang et al., 2011). It decomposes dissolved organic impurities under UV irradiation (Colmenares et al., 2015) and exhibits antibacterial effects (Hossain et al., 2014), in particular in the case of *E.coli* and *S.aureus* (Jaisai et al., 2012). At the same time ZnO is considered safe to people, being added to breakfast cereals and nutrition drinks. In the form of nanoparticles, it was proposed for antimicrobial food packaging (Paisoonsin et al., 2013).

In view of the above arguments, an assumption was made that hybrid polypropylene – zinc oxide nanorod filters shall offer significant improvement in separation characteristics of nonwoven systems.

2. EXPERIMENTAL

Nonwoven filter medium (Amazon Filters Ltd.) in the form of 1 mm thick flat sheets obtained via melt-blow method from polypropylene (PP) homopolymer (Borealis Borflow HL504FB) was used for fabrication of a hybrid material. Distribution of fibre diameters was determined using images taken with scanning electron microscope Hitachi TM1000. Porosity of nonwoven was calculated by weighing specimens of material of known dimensions, using the density of Borealis Borflow HL504FB supplied by its producer (0.95 g/cm^3).

The hybrid material was obtained by means of a three-step process involving: a) plasma treatment of raw nonwoven, b) coating of PP fibres with ZnO nanoparticles, and c) homogenic growth of ZnO nanorods. The polypropylene nonwoven has been treated by a plasma discharge to improve wettability and adhesion of ZnO nanoparticles used as growth initiators to the surface of polymer. The process was conducted in DIONEX Series 2000 reactor with radio frequency plasma generator in oxidizing atmosphere.

Fourier transform infrared spectroscopy (FTIR) was used to determine functional groups introduced onto the surface of fibres as a result of plasma treatment. Samples of raw nonwoven and plasma treated nonwoven were placed upon the diamond attenuated total reflectance (ATR) crystal. Spectra were recorded utilizing Nicolet iS50 spectrometer by averaging 32 signals recorded with resolution of 4 cm^{-1} in range of $4000\text{-}600 \text{ cm}^{-1}$.

Zinc oxide nanoparticles, which are initiators for nanorod growth, were synthesized in isopropanol from zinc acetate and sodium hydroxide. Solutions at concentrations of 1 mM and 15 mM, respectively, were prepared under continuous stirring at $50 \text{ }^\circ\text{C}$. After cooling to room temperature zinc acetate solution was diluted and sodium hydroxide solution was added in dropwise manner for initiation of nucleation. Dispersion of nanoparticles was assured by 2 h of stirring at $60 \text{ }^\circ\text{C}$. In the next step nanoparticles were settled on the fibres by immersion of nonwoven in the dispersion. This was followed by drying at $50 \text{ }^\circ\text{C}$. All these steps were repeated three times.

A directional growth of ZnO nanoparticles on fibres into nanorods with a high aspect ratio was conducted in a water solution of hexa(methylenetetramine) and zinc nitrate at concentrations of 4.5 mM and 3 mM, respectively. Mechanical stirring was employed to assure a uniform concentration of reagents. The solution of reagents was heated to $90 \text{ }^\circ\text{C}$ in oil bath. External filter was used to separate zinc oxide particles crystallizing in the solution. Process of growth lasted 5 h. After that, samples were washed in distilled water to remove by-products and dried at $30 \text{ }^\circ\text{C}$.

Results of each modification steps were verified using a high resolution scanning electron microscope (HR-SEM) Hitachi SU8000. Samples of nonwovens were taken from random locations and for each sample fibres from different layers of nonwoven were characterized in terms of coating density and morphology of zinc oxide particles.

Measurements of specific surface area (SSA) were conducted by BET method using Micrometric ASAP 2010 system. Before measurements gases from the surface of samples were desorbed in vacuum at a temperature of 80 °C (6 hours) followed by rinsing in pure helium. Specific surface area was calculated from Brunauer-Emmet-Teller equation. Phase compositions and contribution of ceramic phase in the modified filter were presented elsewhere (Colmenares et al., 2015). Zeta potentials for raw PP nonwoven and PP-ZnO filter were determined based on streaming potential measurements conducted using electrokinetic analyser Anton Paar SurPASS. Measurements were performed at temperature of 25 °C with addition of potassium chloride electrolyte (1 mM) in pH range from 3 to 11 (pH was controlled by addition of hydrochloric acid or sodium hydroxide with concentrations of 0.5 M). Measured values of streaming potential were converted to zeta potential using Faibrother-Mastin method.

Aerosol filtration efficiency of raw polypropylene and the hybrid nonwoven were examined using Palas Nano MFP plus test system. Aerosol was generated with 1% water solution of KCl. A distribution of particle sizes is presented in Fig. 1. It had a log-normal type with maximum in the range of 50-75 nm (25.6%) with a mean value of about 130 nm. More than 93% of particles had a diameter smaller than 250 nm. Linear velocity of aerosol during dust loading was 0.2 m/second. Fractional efficiency was calculated as a difference between number of particles with given size with and without presence of filter in test chamber.

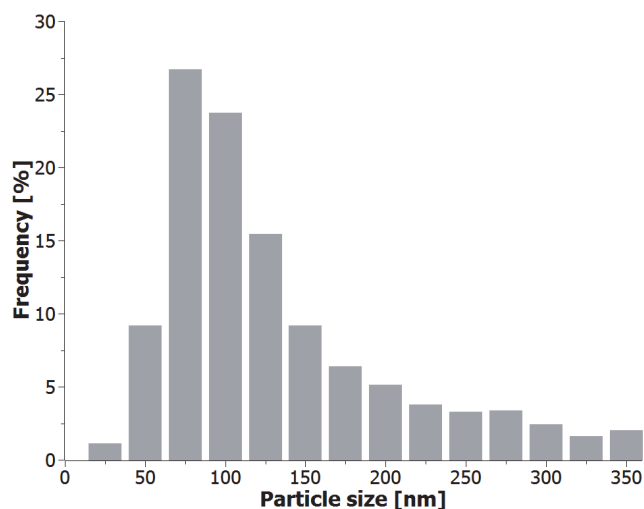


Fig. 1. Size distribution of KCl particles used in aerosol filtration test

The effect of the applied modification on water filtration efficiency was examined using setup presented in Fig. 2.

Six layers of tested filter media were placed in stainless steel housing separated from each other using spacers. Two aqueous dispersions were used for filtration tests:

- polyethyleneimine (PEI) stabilized CuO particle dispersion with mean size of 0.93 μm and zeta potential value of +32.1 mV;
- SiO₂ particle dispersion with mean size of 4.39 μm and zeta potential value of –29.0 mV.

Circulation of the test dispersion during the test was provided by the peristaltic pump. Flow of dispersion was set at the level of 1.6 ml/s – this corresponds to a standard flow through 10-inch cartridge filter (600 l/h) after recalculation for smaller area of the samples.

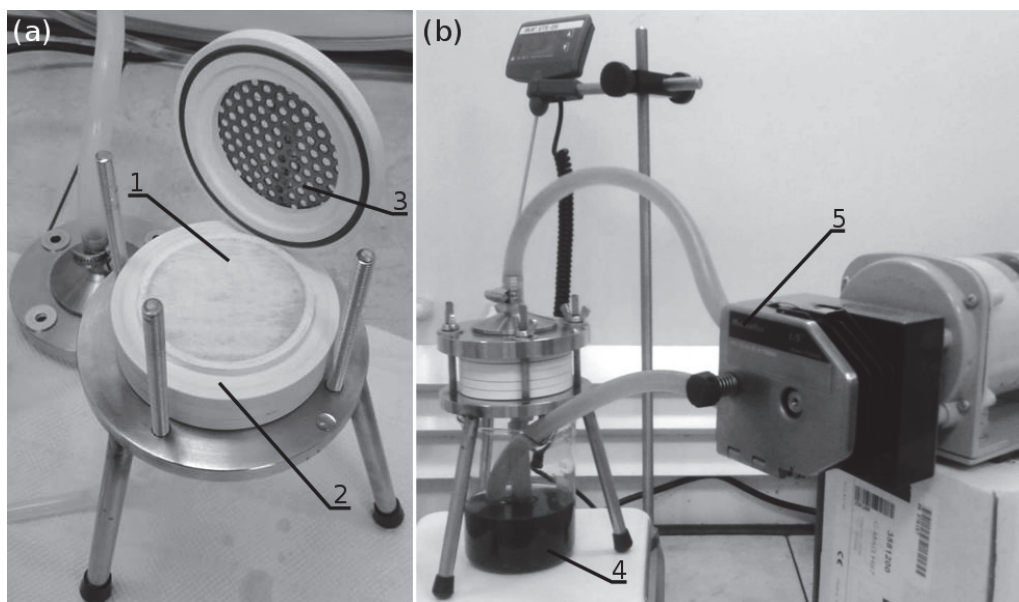


Fig. 2. Equipment used for water filtration tests: housing for filter media (a) and setup during operation (b); 1 - sample of filter media, 2 - spacer with seal, 3 - support for nonwoven, 4 - test dispersion, 5 - peristaltic pump

3. RESULTS

The distribution of fibre diameters of PP nonwoven filter media used as a matrix is presented in Fig. 3. It can be seen that the distribution is broad with two maximums at 9-11 μm (20.4% of fibres) and 13-15 μm (18.0% of fibres). More than 94% of the fibres have diameters lower than 20 μm and 3.9% of them are in sub-micrometric range. The average diameter of fibre is 11.1 μm with standard deviation of 5.5 μm . The porosity was estimated at 94%.

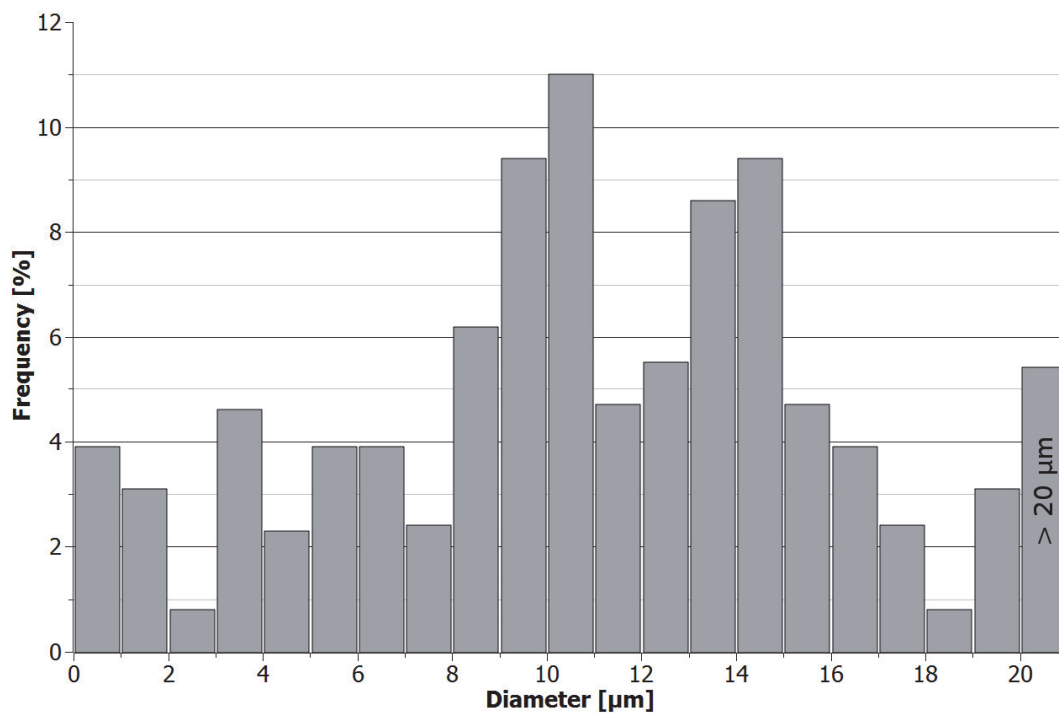


Fig. 3. The distribution of fibre sizes for PP nonwoven

Measurements of contact angles for water droplets, conducted using goniometer, showed that plasma treatment allowed to improve wettability of nonwoven (Fig. 4) with a contact angle decreasing from 135 ± 6 for the initial material to 105 ± 6 degree after the modification.

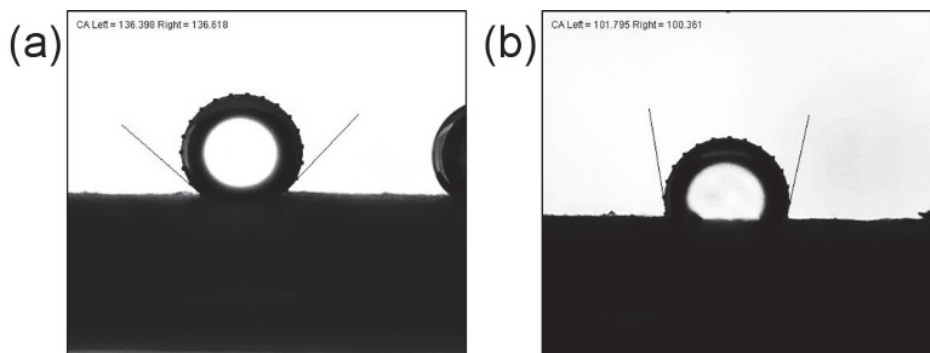


Fig. 4. Contact angles of water droplets on PP nonwovens without (a) and after 5 minutes of 50 W plasma discharge in oxidizing atmosphere (b)

FTIR spectra of PP nonwoven and nonwoven after plasma treatment are presented in Fig. 5. Spectrum obtained for PP nonwoven is typical for a non-crystalline polypropylene (Farrukh, 2012) and contains peaks characteristic for CH_2 - group (2916 cm^{-1} , 2841 cm^{-1}), $>\text{CH}$ - group (1170 cm^{-1} , 975 cm^{-1} , 899 cm^{-1} , 841 cm^{-1} , 810 cm^{-1}) and $-\text{CH}_3$ group (2959 cm^{-1} , 2881 cm^{-1} , 1460 cm^{-1} , 1376 cm^{-1}). In the plasma treated material, peaks are revealed (Paisoonsin et al., 2013; Wanke et al., 2011) characteristic for hydroxyl group $-\text{OH}$ (3395 cm^{-1} , 3190 cm^{-1}) and carbonyl group $>\text{C}=\text{O}$ (1650 cm^{-1}). A peak representing carbon dioxide adsorbed on the surface of material was also observed (2360 cm^{-1}).

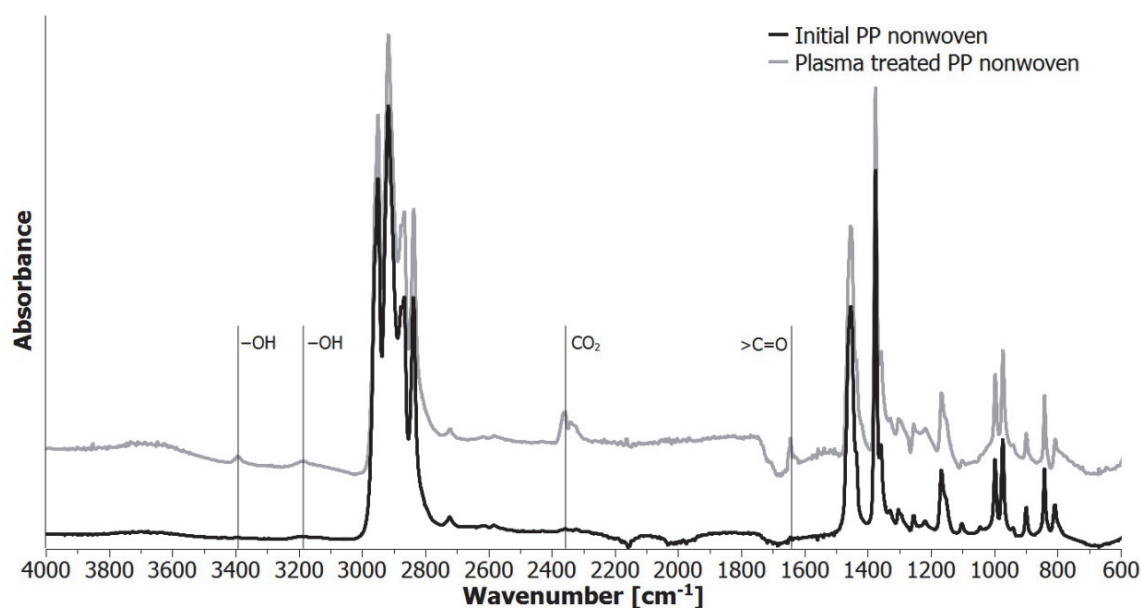


Fig. 5. FTIR spectra of raw PP nonwoven and nonwoven treated by plasma discharge

SEM images of fibres after the deposition and the immobilization of ZnO nanoparticles are shown in Fig. 6. There is a clear difference between fibres with and without plasma treatment. In the case of untreated fibres (Fig. 6a) particles tend to form agglomerates probably due to droplet formation during drying. As evidenced by Fig. 6b fibres after plasma modification are covered by much more uniform layer of ZnO nanoparticles. This rationalizes the use of plasma treated nonwoven for growing ZnO nanorods on fibres (İkizler and Peker, 2014).

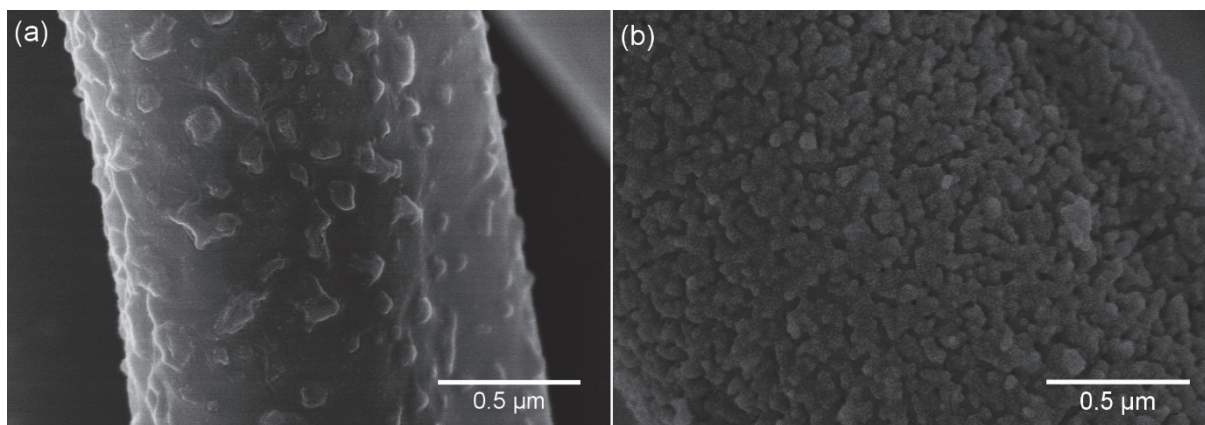


Fig. 6. SEM images of fibres without (a) and with plasma treatment (b) after settling of zinc oxide nanoparticles

SEM images of the ZnO rods grown on fibres are presented in Fig. 7. The rods form dense and uniform structure covering entire surface of fibres, although rods tend to be shorter at deeper layers of material. The diameters of rods range from 10 to 70 nm with maximum in the range of 30-50 nm (53.0% of rods). An average diameter is 38 nm with standard deviation equal to 13 nm. Average distance between adjacent rods is 119 ± 42 nm.

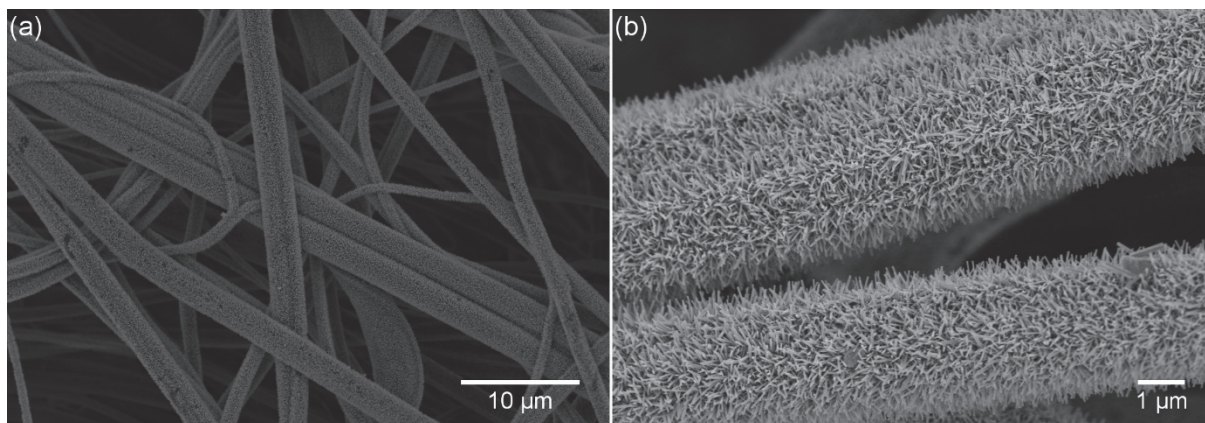


Fig. 7. SEM images of hybrid material obtained after hydrothermal growth of ZnO rods on plasma treated PP nonwoven

Due to the high porosity and limited size of specimen chamber it was impossible to obtain exact value of specific surface area of raw PP nonwoven. It was, however, lower than $0.1 \text{ m}^2/\text{g}$ – the apparatus threshold value. For PP-ZnO hybrid material the measured specific surface area was $0.853 \pm 0.026 \text{ m}^2/\text{g}$, at least eight times higher than that of the raw nonwoven. Zeta potential measurement showed that both materials revealed high, negative charge in water at neutral pH. The zeta potentials for PP nonwoven and PP-ZnO hybrid material were -37.7 mV and -49.4 mV , respectively.

Results of aerosol filtration efficiency tests for both filter media are presented in Fig. 8. In the case of PP nonwoven decrease in filtration efficiency for MPPS particles can be noted. For particles with size of 0.2 µm fractional efficiency achieves its minimum at the level of 65%. For the hybrid material the decrease in fractional efficiency for MPPS particles is much lower and even in its minimum is above 95%. The measured pressure drops were at the level of $27.5 \pm 0.6 \text{ Pa}$ and $30.6 \pm 1.3 \text{ Pa}$ for raw nonwoven and hybrid material, respectively.

The results of water filtration tests are presented in Fig. 9. In the case of CuO particles the dispersion after 5 minutes of the filtration 0.8% and 4.9% of initial solid matter mass was removed for PP nonwoven and PP-ZnO hybrid material, respectively. After 60 minutes it was 7.8% and 26.9%, respectively. In the case of bigger SiO_2 particles during the first 5 minutes of the filtration about 40% of

initial particle mass was removed for both materials, while in the following 5 minutes it was only 10%. After 60 minutes 70.0% and 83.3% of particle mass was removed using PP nonwoven and PP-ZnO hybrid material, respectively.

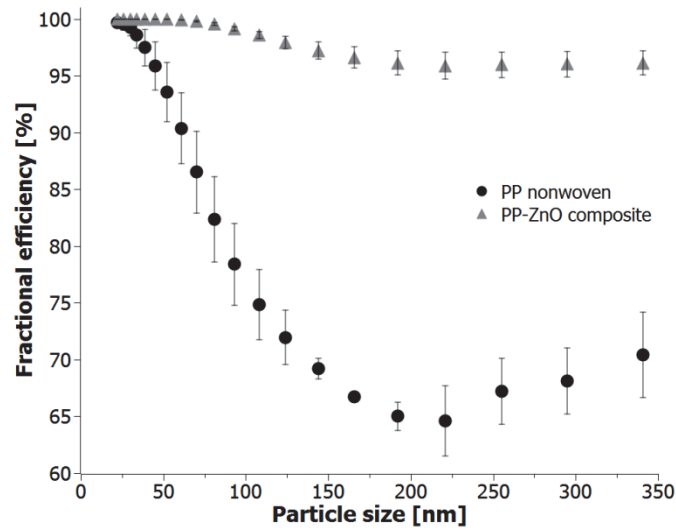


Fig. 8. Results of aerosol filtration efficiency tests obtained for raw PP nonwoven and hybrid material

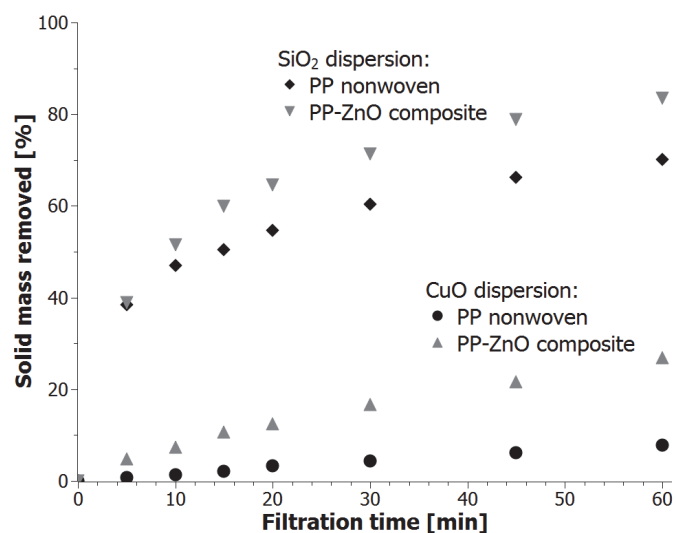


Fig. 9. Solid mass removed from aqueous dispersions of SiO₂ and CuO particles during 60 min of filtration

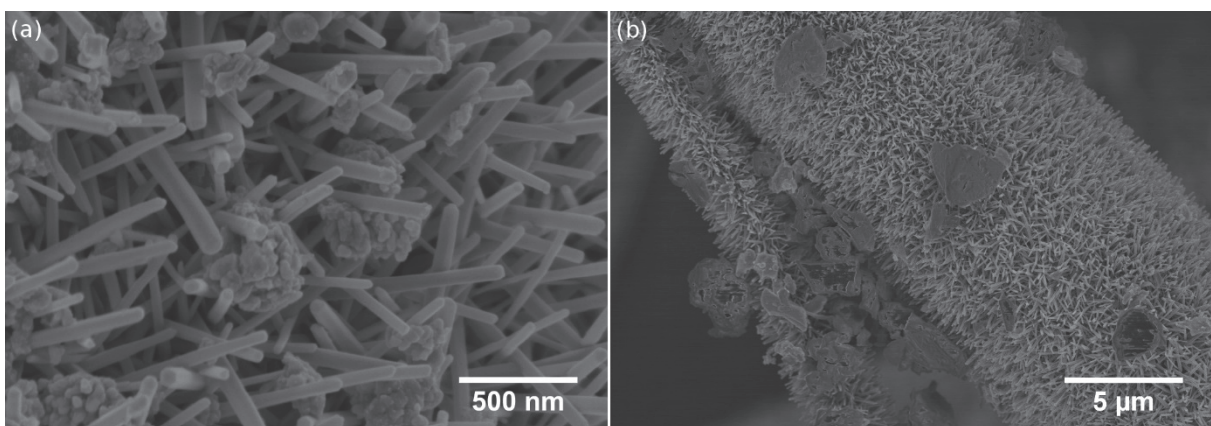


Fig. 10. Solid matter deposited on the surface of PP-ZnO hybrid material during water filtration tests: CuO (a) and SiO₂ (b) particles

SEM images of solid particles deposited on the surface of hybrid material are presented in Fig. 10. As can be seen CuO particles penetrate between ZnO rods, while much bigger SiO₂ particles deposit on the top part of the rods.

4. DISCUSSION

Hydrothermal method of ZnO structure growth was successfully used to obtain fibrous filter media with high specific surface area and high porosity. The modification process can be viewed as a post processing of a melt blown PP nonwoven. Thereby, no modifications to already existing production line are needed, which is a great advantage simplifying commercialization.

Plasma treatment of PP nonwoven resulted in an increase of free surface energy of raw material and removal of contaminants that originated from manufacturing process. During melt blowing process fibres are cooled using water mist which accelerates their solidification. When some contaminants i.e. oil drops are present in the mist they can locally change surface energy of fibres and thus cause problems during the settling of growth initiators. The proposed plasma treatment improves wettability of PP nonwoven assuring a more uniform deposition of growth initiators on fibres, and in turn, uniform distribution of ZnO rods. However, the length of rods is lower for fibres located in deeper layers of the nonwoven and at some distance from the surface, fibres were covered only by ZnO nanoparticles. This non-uniformity can be dealt with by stimulating the flow of reagents through the whole volume of filter media during growth phase.

The development of zinc oxide rods increased the surface area of the filter, allowing to achieve improved filtration efficiencies in both aerosol and water dispersions in filtration tests. One should note also only a slight difference in pressure drop in aerosol filtration test due to the fact that the modification had no influence on macroscopic structure of the filter. As can be seen from SiO₂ dispersion filtration test, application of PP-ZnO hybrid material gives no advantage against PP nonwoven when particles larger than MPPS range are being filtered. Such a difference becomes visible when filtered dispersions consisted mostly of particles with sizes close to MPPS range. In the case of CuO dispersions, the hybrid material revealed improved filtration efficiency from the very beginning of the process. It can also be seen that in the case of CuO dispersions, the difference between both materials was increasing linearly during the entire experiment.

Results presented in the literature indicate that the new hybrid filter may find potential application in ventilation and air conditioning systems or as a personal respiratory protection when microbiological hazard needs to be considered due to the antibacterial activity of ZnO (Ivanova et al., 2012; Li et al., 2008; Li et al., 2013; Pogodin et al., 2013; Tam et al., 2008).

5. CONCLUSIONS

Hybrid filter media consisting of PP nonwoven and ZnO structures with high aspect ratio were successfully obtained via low temperature hydrothermal method. Modification process was designed as a post-treatment of commercially produced filter to simplify potential commercialization. It was shown that applied plasma treatment of base polypropylene nonwoven resulted in 30 degree reduction of wetting angle, which allowed for more uniform distribution of growth initiators on the surface of fibres. This layer has crucial impact on morphology of obtained ZnO rods. Due to the concurrency mechanism, the more dense and uniform is layer of growth initiators, the finer rods can be obtained as a result of hydrothermal growth. Conducted application tests showed that hybrid material revealed improved filtration properties compared to a standard PP nonwoven. What is important to note, while fractional filtration efficiency for aerosol particles with diameter of 0.2 μm increased by 30%,

measured initial pressure drop increased only slightly by about 3 Pa. This result suggests that it may be possible to create a highly effective filter by increasing the thickness of such hybrid material, which should have much lower pressure drop compared to commonly used HEPA filters.

Project supported by a grant from Switzerland through the Swiss Contribution to the enlarged European Union. Authors are also grateful to Juan Carlos Colmenares from Polish Academy of Sciences for help with FTIR analysis.

REFERENCES

- Ahamed M., AlSalhi M.S., Siddiqui M.K.J., 2010. Silver nanoparticle applications and human health. *Clin. Chim. Acta*, 411, 1841–1848. DOI: 10.1016/j.cca.2010.08.016.
- Apalangya V., Rangari V., Tiimob B., Jeelani S., Samuel T., 2014. Development of antimicrobial water filtration hybrid material from bio source calcium carbonate and silver nanoparticles. *Appl. Surf. Sci.*, 295, 108–114. DOI: 10.1016/j.apsusc.2014.01.012.
- Ates T., Tatar C., Yakuphanoglu F., 2013. Preparation of semiconductor ZnO powders by sol–gel method: Humidity sensors. *Sens. Actuators A: Phys.*, 190, 153–160. DOI: 10.1016/j.sna.2012.11.031.
- Baek S.-H., Kim S.-B., Shin J.-K., Kim J. H., 2012. Preparation of hybrid silicon wire and planar solar cells having ZnO antireflection coating by all-solution processes. *Sol. Energy Mater. Sol. Cells*, 96, 251–256. DOI: 10.1016/j.solmat.2011.10.007.
- Ben-Sasson M., Lu X., Bar-Zeev E., Zodrow K.R., Nejati S., Qi G., Elimelech M., 2014. In situ formation of silver nanoparticles on thin-film composite reverse osmosis membranes for biofouling mitigation. *Water Res.*, 62, 260–270. DOI: 10.1016/j.watres.2014.05.049.
- Chang Q., Zhou J., Wang Y., Liang J., Zhang X., Cerneaux S., Dong Y., 2014. Application of ceramic microfiltration membrane modified by nano-TiO₂ coating in separation of a stable oil-in-water emulsion. *J. Membr. Sci.*, 456, 128–133. DOI: 10.1016/j.memsci.2014.01.029.
- Chen K.J., Hung F.Y., Chang S.J., Young S.J., 2009. Optoelectronic characteristics of {UV} photodetector based on ZnO nanowire thin films. *J. Alloys Compd.*, 479, 674–677. DOI: 10.1016/j.jallcom.2009.01.026.
- Chen R., Bayon Y., Hunt J.A., 2012. Preliminary study on the effects of ageing cold oxygen plasma treated PET/PP with respect to protein adsorption. *Colloids Surf., B: Biointerfaces*, 96, 62–68. DOI: 10.1016/j.colsurfb.2012.03.019.
- Choi H.-S., Vaseem M., Kim S.G., Im Y.-H., Hahn Y.-B., 2012. Growth of high aspect ratio ZnO nanorods by solution process: Effect of polyethyleneimine. *J. Solid State Chem.*, 189, 25–31. DOI: 10.1016/j.jssc.2011.12.008.
- Coen M.C., Dietler G., Kasas S., Gröning P., 1996. {AFM} measurements of the topography and the roughness of {ECR} plasma treated polypropylene. *Appl. Surf. Sci.*, 103, 27–34. DOI: 10.1016/0169-4332(96)00461-8.
- Colmenares J.C., Kuna E., Jakubiak S., Michalski J., Kurzydłowski K.J., 2015. Polypropylene nonwoven filter with nanosized ZnO rods: Promising hybrid photocatalyst for water purification. *Appl. Catal. B: Environ.*, 170–171, 273–282. DOI: 10.1016/j.apcatb.2015.01.031.
- Cruz M.C., Ruano G., Wolf M., Hecker D., Vidaurre E.C., Schmittgens R., Rajal V.B., 2014. Plasma deposition of silver nanoparticles on ultrafiltration membranes: Antibacterial and anti-biofouling properties. *Chem. Eng. Res. Des.*, 94, 524–537. DOI: 10.1016/j.cherd.2014.09.014.
- Farrukh M.A., 2012. *Advanced aspects of spectroscopy*. InTech. DOI: 10.5772/2757.
- Hossain F., Perales-Perez O.J., Hwang S., Román F., 2014. Antimicrobial nanomaterials as water disinfectant: Applications, limitations and future perspectives. *Sci. Total Environ.*, 466–467, 1047–1059. DOI: 10.1016/j.scitotenv.2013.08.009.
- İkizler B., Peker S.M., 2014. Effect of the seed layer thickness on the stability of ZnO nanorod arrays. *Thin Solid Films*, 558, 149–159. DOI: 10.1016/j.tsf.2014.03.019.
- Ivanova E.P., Hasan J., Webb H.K., Truong V.K., Watson G.S., Watson J.A., Crawford R.J., 2012. Natural bactericidal surfaces: mechanical rupture of *Pseudomonas aeruginosa* cells by cicada wings. *Small*, 8, 2489–2494. DOI: 10.1002/sml.201200528.

- Jackiewicz A., Podgórski A., Gradon L., Michalski J., 2013. Nanostructured media to improve the performance of fibrous filters. *Kona Powder Part. J.*, 30, 244–255. DOI: 10.14356/kona.2013023.
- Jaisai M., Baruah S., Dutta J., 2012. Paper modified with ZnO nanorods – antimicrobial studies. *Beilstein J. Nanotechnol.*, 3, 684–691. DOI: 10.3762%2Fbjnano.3.78.
- Jaleh B., Parvin P., Wanichapichart P., Saffar A.P., Reyhani A., 2010. Induced super hydrophilicity due to surface modification of polypropylene membrane treated by {O₂} plasma. *Appl. Surf. Sci.*, 257, 1655–1659. DOI: 10.1016/j.apsusc.2010.08.117.
- Kaegi R., Sinnet B., Zuleeg S., Hagendorfer H., Mueller E., Vonbank R., Burkhardt M., 2010. Release of silver nanoparticles from outdoor facades. *Environ. Pollut.*, 158, 2900–2905. DOI: 10.1016/j.envpol.2010.06.009.
- Kenanakis, G., Vernardou, D., Katsarakis, N., 2012. Light-induced self-cleaning properties of ZnO nanowires grown at low temperatures. *Appl. Catal. A: General*, 411–412(0), 7–14. DOI: 10.1016/j.apcata.2011.09.041.
- Kwon Y. Bin, Shin S.W., Lee H.-K., Lee J.Y., Moon J.-H., Kim J.H., 2011. Formation of ZnO thin films consisting of nano-prisms and nano-rods with a high aspect ratio by a hydrothermal technique at 60 °C. *Curr. Appl Phys.*, 11, S197 – S201. DOI: 10.1016/j.cap.2010.11.086.
- Li M., Lin D., Zhu L., 2013. Effects of water chemistry on the dissolution of ZnO nanoparticles and their toxicity to *Escherichia coli*. *Environ. Pollut.*, 173, 97–102. DOI: 10.1016/j.envpol.2012.10.026.
- Li Q., Mahendra S., Lyon D.Y., Brunet L., Liga M.V, Li D., Alvarez P.J.J., 2008. Antimicrobial nanomaterials for water disinfection and microbial control: Potential applications and implications. *Water Res.*, 42, 4591–4602. DOI: 10.1016/j.watres.2008.08.015.
- Li Y.P., Shi W., Li S.Y., Lei M.K., 2012. Transition of water adhesion on superhydrophobic surface during aging of polypropylene modified by oxygen capacitively coupled radio frequency plasma. *Surf. Coat. Technol.*, 213, 139–144. DOI: 10.1016/j.surfcoat.2012.10.037.
- Minh V., Tuan L.A., Huy T.Q., Hung V.N., Quy N.Van., 2013. Enhanced {NH₃} gas sensing properties of a QCM sensor by increasing the length of vertically orientated ZnO nanorods. *Appl. Surf. Sci.*, 265, 458–464. DOI: 10.1016/j.apsusc.2012.11.028.
- Nayeri F.D., Soleimani E.A., Salehi F., 2013. Synthesis and characterization of ZnO nanowires grown on different seed layers: The application for dye-sensitized solar cells. *Renewable Energy*, 60, 246–255. DOI: 10.1016/j.renene.2013.05.006.
- Paisoonsin S., Pornsunthorntawe O., Rujiravanit R., 2013. Preparation and characterization of ZnO-deposited DBD plasma-treated {PP} packaging film with antibacterial activities. *Appl. Surf. Sci.*, 273, 824–835. DOI: 10.1016/j.apsusc.2013.03.026.
- Pishbin F., Mouriño V., Gilchrist J.B., McComb D.W., Kreppel S., Salih V., Boccaccini A.R., 2013. Single-step electrochemical deposition of antimicrobial orthopaedic coatings based on a bioactive glass/chitosan/nano-silver composite system. *Acta Biomater.*, 9, 7469–7479. DOI: 10.1016/j.actbio.2013.03.006.
- Podgórski A., Bałazy A., Gradoń L., 2006. Application of nanofibers to improve the filtration efficiency of the most penetrating aerosol particles in fibrous filters. *Chem. Eng. Sci.*, 61, 6804–6815. DOI: 10.1016/j.ces.2006.07.022.
- Pogodin S., Hasan J., Baulin V.A., Webb H.K., Truong V.K., Nguyen T.H.P., Ivanova E.P., 2013. Biophysical model of bacterial cell interactions with nanopatterned cicada wing surfaces. *Biophys. J.*, 104, 835–840. DOI: 10.1016/j.bpj.2012.12.046.
- Sutherland K., 2011. Filtration markets: The European market for filtration equipment. *Filtration + Separation*, 48, 32–35. DOI: 10.1016/S0015-1882(11)70084-2.
- Tam K.H., Djurišić A.B., Chan C.M.N., Xi Y.Y., Tse C.W., Leung Y.H., Au D.W.T., 2008. Antibacterial activity of ZnO nanorods prepared by a hydrothermal method. *Thin Solid Films*, 516, 6167–6174. DOI: 10.1016/j.tsf.2007.11.081.
- Wanke C.H., Feijó J.L., Barbosa L.G., Campo L.F., de Oliveira R.V. B., Horowitz F., 2011. Tuning of polypropylene wettability by plasma and polyhedral oligomeric silsesquioxane modifications. *Polymer*, 52, 1797–1802. DOI: 10.1016/j.polymer.2011.01.064.
- Yin M., Liu M., Liu S., 2014. Diameter regulated ZnO nanorod synthesis and its application in gas sensor optimization. *J. Alloys Compd.*, 586, 436–440. DOI: 10.1016/j.jallcom.2013.10.081.
- Zhang D., Chen L., Zang C., Chen Y., Lin H., 2013. Antibacterial cotton fabric grafted with silver nanoparticles and its excellent laundering durability. *Carbohydr. Polym.*, 92, 2088–2094. DOI: 10.1016/j.carbpol.2012.11.100.
- Zhang H., Chen B., Jiang H., Wang C., Wang H., Wang X., 2011. A strategy for ZnO nanorod mediated multi-mode cancer treatment. *Biomaterials*, 32, 1906–1914. DOI: 10.1016/j.biomaterials.2010.11.027.

Zhou K., Dong C., Zhang X., Shi L., Chen Z., Xu Y., Cai H., 2015. Preparation and characterization of nanosilver-doped porous hydroxyapatite scaffolds. *Ceram. Int.*, 41(1, Part B), 1671–1676. DOI: 10.1016/j.ceramint.2014.09.108.

Received 15 February 2016

Received in revised form 18 June 2016

Accepted 20 June 2016